

SELECTION AND DESIGN OF TILTING PAD AND FIXED LOBE JOURNAL BEARINGS FOR OPTIMUM TURBOROTOR DYNAMICS

by

John C. Nicholas

Analytical Engineer, Rotor Dynamics Analysis

and

R. Gordon Kirk

Supervisor, Rotor Dynamics Analysis

Ingersoll-Rand Company

Phillipsburg, New Jersey



John C. Nicholas received his B.S.A.E. from the University of Pittsburgh in 1968, and his M.S.M.E. from Northwestern University in 1969. After two years in the U.S. Army, he received his Ph.D. in 1977 from the University of Virginia.

While at Virginia, he specialized in finite element bearing dynamics and rotor-bearing system analysis. His work, which was part of an ERDA contract, included pressure dam and tilting pad bearing design optimizations for improved turborotor stability. After receiving his Ph.D., he was an assistant professor in Virginia's M.E. department.

Currently, he is a member of the Rotor Dynamics Analysis Group at Ingersoll-Rand. His work includes computer program development and design optimization for fixed lobe and tilting pad bearings. He is also involved with turbomachinery design and analysis.

Dr. Nicholas has authored more than 10 technical articles in rotor dynamics and bearing design. He is also co-authoring a book on fluid film lubrication.



R. Gordon Kirk is supervisor of the Rotor Dynamics Analysis Section of the Turbo Products Division at Ingersoll-Rand Company. He is responsible for rotor-bearing design and analysis for all Turbo Products compressors, turbines, and hot gas expanders.

A native of Coeburn, Virginia, Dr. Kirk attended Clinch Valley College where he received an Associate Degree in Engineering. He studied mechanical engineering at the University of Virginia where he received a B.S. degree with high distinction in 1967, an M.S. degree in 1969, and a Ph.D. in 1972.

While working toward his Ph.D., he taught mechanical engineering at the University of Virginia, and as a research engineer, worked on a NASA contract for transient analysis of flexible rotor-bearing systems. After receiving his Ph.D., he worked for Pratt and Whitney Aircraft in East Hartford, Connecticut, in rotor dynamics analysis and transient response analysis.

In 1975, he joined Ingersoll-Rand as a senior analyst in the development group, and continued to develop expertise in rotor dynamics analysis and investigate the influence of oil seals on the stability of compressor rotors. His work resulted in a patent for a unique bearing support system. Further work on oil seals

resulted in a second patent for stabilized cone oil seals.

Dr. Kirk is the author of more than 20 technical papers and reports on rotor-bearing design and analysis.

ABSTRACT

Current trends in bearing designs for turbomachinery are reviewed in terms of manufacturing tolerances and overall design considerations. Discussion of both fixed bore and tilting pad bearings with regard to forced response and stability leads to conclusions and recommendations for optimum rotor dynamic performance of turborotors. Examples of design studies of actual rotor systems are presented and discussed to illustrate the optimization procedures and recommendations.

INTRODUCTION

The selection and design of fluid-film bearings for turbomachinery has become extremely important for both the O.E.M. (original equipment manufacturer) and end-users. The O.E.M. is concerned with the expedient testing, shipment, and successful field operation of their product. Typically, the end-user has a product that is dependent on the satisfactory operation of the turbomachinery to either drive the process equipment or to compress, pump, or otherwise perform its given process function.

Improvements in monitoring vibration levels have enabled the end-user to sometimes forecast potential downtime and thus save time and money with unscheduled shutdowns. The collection of data on large numbers of machines has thus enabled both the O.E.M. and the end-user to develop acceptance criteria for rotor synchronous and non-synchronous vibration levels. The occurrence of high synchronous response is usually the result of poor or improper balance or rotor building procedures, but it can also be traced to a marginal bearing design in regards to effective system damping levels. The occurrence of sub-synchronous vibration is typically an indication of a bearing or oil seal induced instability that can be either a mild and acceptable level or a potentially dangerous form of response.

Bearings and oil seals are not the only source of sub-synchronous vibration, and its occurrence does not necessarily indicate improper bearing or oil seal design. Other examples of sub-synchronous vibration sources are light rubs, steam whirl, aerodynamic excitation from turborotor stages or labyrinths, internal friction, entrapped fluids, piping resonance, acoustic standing wave phenomena in associated piping, loose shaft elements, loose bearing inserts or housings, aerodynamic excitation arising from turbulence or vortex shedding from piping

or turbo-rotor stages, and operation in a region close to or in a condition of surge. The later forms of instability forcing functions are not easily modeled into commonly available rotor dynamics computer programs, but system sensitivity to this type of phenomena can be studied by the generally accepted cross-coupled stiffness mechanism.

Calculation procedures and design guides for bearings and oil seals are currently being developed to the point that satisfactory predictions can be made in the original design stages of new and/or improved rotor-bearing systems. This capability has been rapidly increasing the interest of the end-user in the analytical prediction of response sensitivity and stability in the early stages of new turbomachinery design. Rigid specifications have thus been prepared by most O.E.M.'s in regard to acceptable rotor dynamics behavior, and equally strict specifications are appearing in current new orders and re-rate studies.

This paper will explore the advantages and disadvantages of standard bearing designs and the shortcomings of the current analytical procedures used to predict rotor vibration levels and stability. Several example design studies are reviewed to demonstrate the influence of the numerous design variations available to the bearing designer. General conclusions are drawn from the specific examples presented.

PRACTICAL DESIGN CONSIDERATIONS FOR FLUID-FILM BEARINGS

Geometric Properties of Various Bearing Designs

The bulk of the published analytic predictions of bearing performance prior to the mid-sixties had been conducted by researchers using the cavitated plain journal bearing model. More recent research has been responsible for publication of design data for more complex insert type bearings and refined data for tilting pad bearings. The use of computer codes for bearing performance has shortened the time required to adequately evaluate rotor system acceptability. The ability to calculate the stiffness and damping properties of a specific bearing design does not, however, assure the designer that the exact bearing can be manufactured. The influence of design tolerances on bearings, and hence rotor dynamics, has become of increasing importance because test stand data is expected to correlate with predicted performance. The designer must therefore consider more than nominal bearing clearance conditions since many rotor designs are sensitive to bearing design tolerances.

A major concern for all bearing designs is the circularity of the bearing profile. The use of "crush" was standard practice in past years to assure satisfactory performance of simple journal bearings. This has been documented to be of equal importance, if not more so, for the axial-groove type insert [1] where crush can effectively preload, and hence stabilize an otherwise unstable design.

Current design tolerances call for bearing clearances to be held to some nominal value with a tolerance of typically plus or minus one mil. Journals below 3 in. (7.62 cm) typically call for a tolerance of 1.5 mils (.0038 cm) or less on the diameter. The realization of the tolerances on the individual components of the journal bearing are of extreme importance for adequate bearing evaluation. Precision ground shafts can be manufactured to a tolerance of 0.5 mils (0.00127 cm) without extreme cost. This then typically leaves 1.5 mils tolerance on the bearing insert/housing fit-up or the tilt pad/housing tolerance stack-up. Individual pad height can be held to .25 mils which

then accounts for 1.0 mils more than the tolerance. This leaves 0.5 mils tolerance for the housing which retains the pads.

Multi-lobe bearings are particularly sensitive to the profile depth of the circumferential taper of each lobe when rotor balance cannot be maintained. Pocket type insert bearings are more forgiving with respect to pocket depth and are therefore more desirable than true lobe bearing designs from that aspect. In addition, pocket type lobe or pressure dam inserts can be designed to have improved stability with regards to oil-whirl or shaft-whip excitation.

The preload factor for tilt pad or lobe bearings is forced to have a range that varies typically by 20-30% for tolerances similar to those indicated above. Allowances must be made for pad curvature or lobe profile [1] when the actual preload values are being calculated.

Thermal Considerations

The calculation of accurate bearing characteristics must consider a proper oil viscosity which can be calculated by considering a flow-heat balance on each pad or lobe of the bearing. Accurate prediction of pad or lobe average temperature must account for pad to pad carry-over and mixing of oil at the leading edge of each pad or lobe. A typical carry-over factor for a 5-pad bearing is in the range of 50-60% of the circulation flow leaving the trailing edge of the former pad. Particular designs must have this factor modified to account for actual oil flow characteristics.

Insert type bearings with feeder slots or grooves and orifice type weep holes for exit flow can be modeled for ideal mixing — considering the oil in, oil out, and circulation flow into the pocket to approximate the heat-flow balance for the insert. Exact solutions are possible, but satisfactory results can be obtained by using plain journal bearing theory friction loss and the flow balance as noted above.

The use of accurate viscosity-temperature information for the lubricant used in the bearing is essential. This information is available from the suppliers, and routines can be written for computer automation of the relationship.

Calculation of hot bearing clearances for power turbines and expanders must be considered in addition to the cold or start-up clearances for such "hot" bearing designs. Shaft differential growth must also be accounted for.

Influence of Bearing Bracket or Support Structure

It is essential to properly account for structural stiffness for heavily loaded bearings having dynamic stiffness values in excess of 3×10^6 lb/in. Typical casing stiffness values can range from $3-15 \times 10^6$ lb/in., and it is therefore necessary to account for these effects in the total system analysis.

Tilting pad bearing design must also consider the influence of the pivot flexibility and stress levels. Application of ball and roller bearing Hertzian stress theory to calculate the effective pivot stiffness for each pad should be considered for larger machines having bearing stiffness levels in excess of 3×10^6 lb/in. Typical pivot stiffness levels can be in the range of $6-10 \times 10^6$ lb/in. and vary according to the loading and type of pivot utilized (i.e., cylindrical, ball, or double curvature).

Machinery designed with a flexible bearing support structure should be statically or dynamically loaded to determine the proper equivalent stiffness such that representative stiffness levels may be used to more accurately predict the system response and stability.

JOURNAL BEARING DESIGNS FOR LOW SPEED AXIAL COMPRESSORS

Axial Compressor Introduction

This section considers the selection and design of journal bearings for heavy, low speed axial compressors where the shaft stiffness is in the same range as the bearing stiffness. The analyses and conclusions are also valid for other types of turbomachinery that fall into this category such as many turbines and hot gas expanders. This type of machine operates below the first bending critical; however, the operating range is usually around the first or second rigid body critical (cylindrical and conical modes). These modes are sometimes referred to as bearing criticals since the bearing stiffness and damping properties have a large influence on the frequency and amplification of the resonance speeds. Furthermore, if the bearing properties are asymmetric, distinct peak amplifications may be observed at different frequencies whose mode shapes correspond very nearly to the cylindrical mode. That is, the first rigid body mode may be observed twice due to the bearings' asymmetric properties. Clearly, since the bearings control these rigid body modes, bearing design is crucial in determining the performance of this class of turbomachinery.

Although the speeds are relatively low for these types of machines, oil whirl may be a problem with fixed lobe bearings. The designer is often faced with the choice of going to a tilt pad design to eliminate the oil whirl or to a modified fixed lobe design that features improved stability characteristics. Since the shaft is relatively rigid for this class of machinery, an improved fixed lobe design often will insure stable operation.

The analyses in this section feature three different axial compressors that range in speed from 3,600 to 5,500 RPM and in weight from 72,102 N (16,210 lbs.) to 21,079 N (4,739 lbs.). Table 1 summarizes the characteristics of these three machines. The objective of these analyses is to investigate the compressor's performance with the standard 3-axial groove bearing and to choose a backup bearing design. This backup may be either a modified fixed lobe (step journal in this case; see Figure 1) or a tilting pad bearing. Both types are considered for all three axials. Table 2 summarizes the parameters for all bearings considered in the analyses.

Stability Analysis, Axial Compressor Number 1

Figure 2 is a stability map for the lightest axial ($W_r = 21079 \text{ N}$, 4,739 lbs.) machine number 1. This compressor has a journal diameter of 13.97 cm (5.5 in.) and an operating speed of 5,500 RPM. The stability analysis uses a transfer matrix approach similar to the method outlined in reference [2]. All destabilizing forces are lumped into one parameter, aerodynamic cross-coupling, Q [2, 3, 4, 5]. This parameter is plotted against the real part of the eigenvalue or the growth factor. The stability threshold is indicated at a growth factor of zero while positive values are unstable.

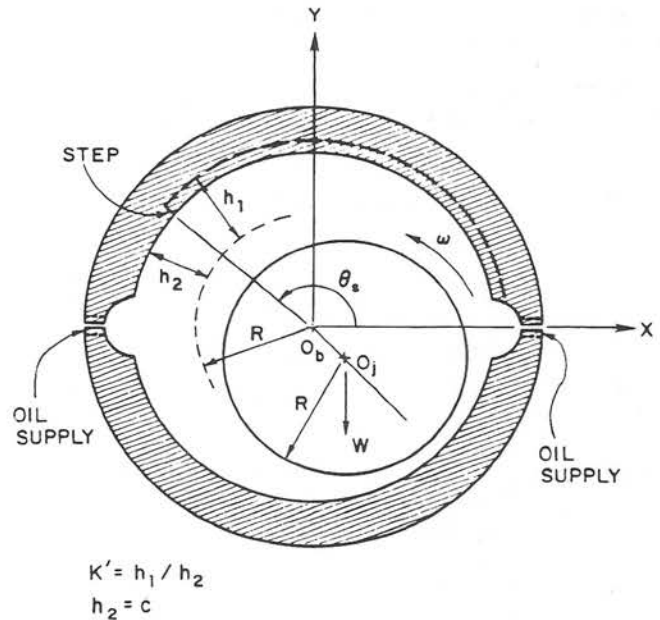


Figure 1. Step Journal or Pressure Dam Bearing.

Three bearings are considered: 3-axial groove, step journal and 4-pad tilting pad. The 3-axial groove design is predicted to be either on the stability threshold or unstable depending on the amount of destabilizing aerodynamic forces present in the compressor. The step bearing design, however, places the compressor into the stable region with a real root of -22 compared to $+4$ for the 3-axial groove bearing ($Q = 1.75 \times 10^4 \text{ N/cm}$, 10^4 lbs/in.). The 4-pad tilt pad bearing design with between pad loading further increases the compressor's stability margin. Two curves are shown in Figure 2 indicating the extreme tolerance range on the bearing clearance and preload (Figure 3). Since damping increases with decreasing preload and/or decreasing bearing clearances, c_b , the $M = .3$, $c_b = .0762 \text{ mm}$ (3.0 mils) bearing provides a larger margin of stability compared to the $M = .5$, $c_b = .127 \text{ mm}$ (5.0 mils) 4-pad design. The compressor goes unstable with all three bearing designs for extremely large values of Q .

Table 2 indicates that for machine number 1, the length to diameter ratio of the 4-pad tilt pad design is less than the L/D ratio for the fixed lobe cases (.45 compared to .55). A decrease in bearing length is necessary for tilt pad bearings if they are to fit into the same housing due to the additional space needed for the shoe retainers and end seals. Figure 4 indicates that as the L/D ratio increases for the 4-pad tilting pad bearing loaded between the pads, damping increases as stiffness decreases. Usually, stiffness and damping either both increase or both decrease. This rare quality probably holds only for this bearing in the moderate Sommerfeld range ($0.1 \leq S \leq 1.0$). Thus, the largest L/D ratio should be used in this case.

TABLE 1. SUMMARY OF AXIAL COMPRESSOR CHARACTERISTICS.

Machine Number	W_r		N (RPM)	N_{cr} (RPM)	L_b		$K_s \times 10^{-6}$		\bar{K}^*
	(lbs)	(N)			(in)	(cm)	(lb/in)	(N/cm)	
1	4739	21079	5500	6000	97	246	2.4	4.2	2.3
2	16210	72102	3600	4780	134	340	5.3	9.3	1.7
3	7118	31661	5500	7500	87	221	5.7	10.0	0.68

*At operating speed using average bearing stiffnesses

TABLE 2. SUMMARY OF BEARING PARAMETERS FOR THE THREE AXIAL COMPRESSORS.

Machine Number	Bearing Type	D		L/D	c, c _b		S*	R _e *	Step Journal		Tilting Pad			
		(in)	(cm)		(mils)	(mm)			K'	θ _s	M	Loading		
1	3-Axial Groove	5.5	13.97	.55	3.0	.0762	.75	272	4.7	120°				
	Step Journal	↓	↓	.55	3.0	.0762	↓	↓						
	4-Pad Tilt	↓	↓	.45	3.0	.0762	↓	↓					.3	Between
	4-Pad Tilt	↓	↓	.45	5.0	.127	↓	↓					.5	Between
2	3-Axial Groove	8.0	20.32	.78	5.5	.1397	.24	442	4.1	120°				
	Step Journal	↓	↓	.78	5.5	.1397	↓	↓						
	4-Pad Tilt	↓	↓	.70	6.0	.1524	↓	↓					.2	Between
	4-Pad Tilt	↓	↓	.70	6.0	.1524	↓	↓					.45	Between
3	3-Axial Groove	6.5	16.51	.77	4.5	.1143	.71	766	4.6	120°				
	Step Journal	↓	↓	.77	↓	↓	↓	↓						
	4-Pad Tilt	↓	↓	.60	↓	↓	↓	↓					.5	Between
	5-Pad Tilt	↓	↓	.60	↓	↓	↓	↓					.5	Between
	5-Pad Tilt	↓	↓	.60	↓	↓	↓	↓	.5	On				

*At Operating Speed

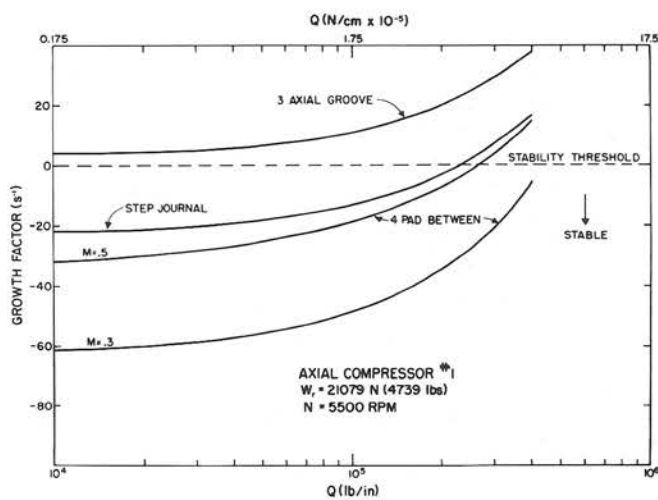


Figure 2. Stability Map, Axial Compressor Number 1.

Vibration Analysis, Axial Compressor Number 2

The second axial compressor listed in Table 1 is the heaviest of three machines weighing 72,102 N (16,210 lbs.) with a 20.32 cm (8.0 in.) journal. Also, the operating speed is lower at 3600 RPM. The operating Sommerfeld number is .24 which is much lower than .75 and .71 for machine numbers 1 and 3, respectively. The stability map for this machine is shown in Figure 5. Similar results are depicted compared to Figure 2. Again, the 3-axial groove bearing operates on the stability threshold while the step journal design moves the margin of stability into the stable region. The 4-pad tilting pad bearing further increases the stability margin. Two different preloads are shown, M = .2 and M = .45. The lowest preload provides the largest stability margin due to the increase in bearing damping.

Figure 6 shows that for S = .24 and increasing L/D ratios, stiffness decreases while damping increases. The increase in

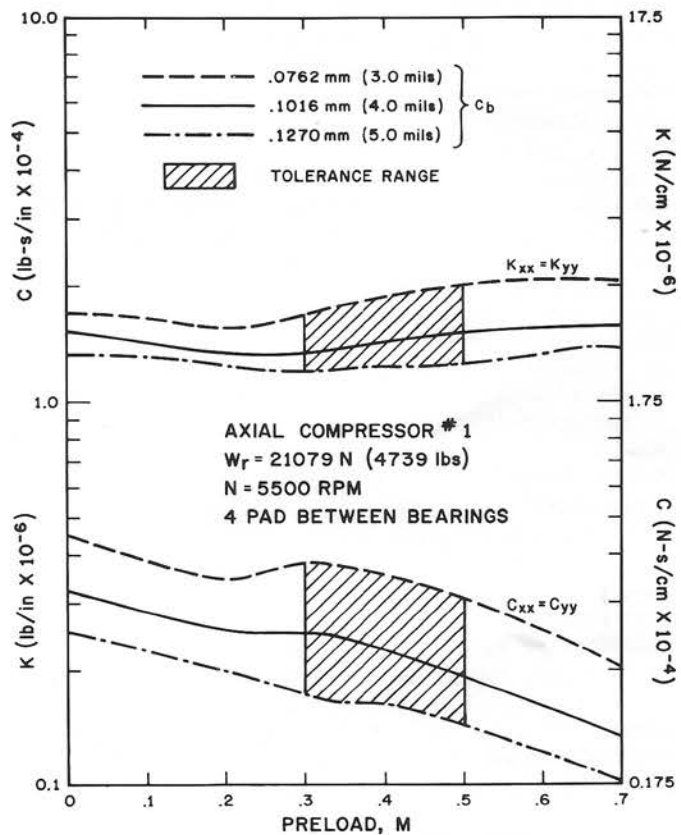


Figure 3. Variation in Stiffness and Damping with Preload and Bearing Clearance, 4-Pad Bearing, D = 13.97 cm, 5.5 in.

damping is not as pronounced as in Figure 4 (S = .75). However, the decrease in stiffness is still beneficial from a stability standpoint since softer bearings allow more bearing damping to combat the destabilizing aerodynamics inboard of the bearings [5]. Again, the largest L/D ratio should be chosen. Additionally, since this compressor is very heavy, concern for

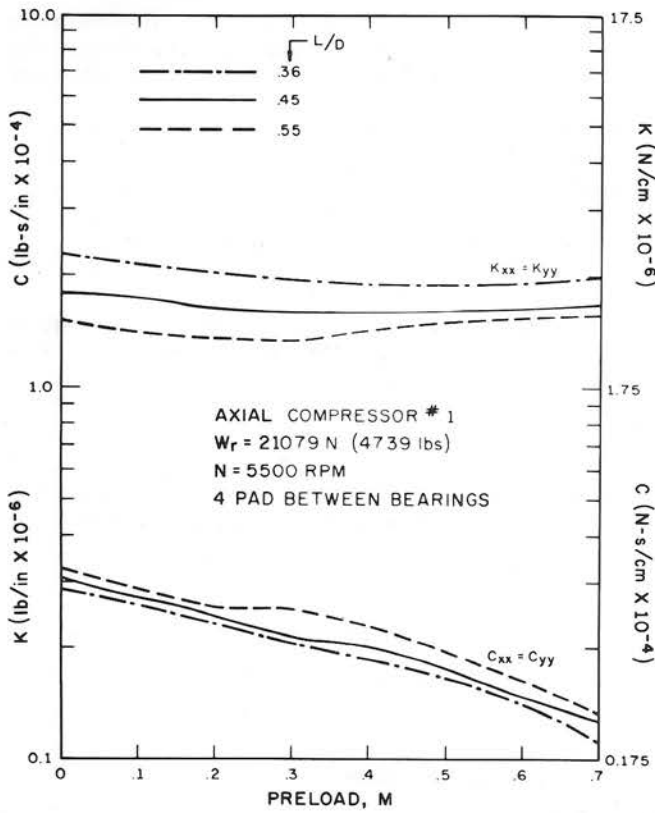


Figure 4. Variation in Stiffness and Damping with Preload and Length to Diameter Ratio, 4-Pad Bearing, $D = 13.97$ cm, 5.5 in.

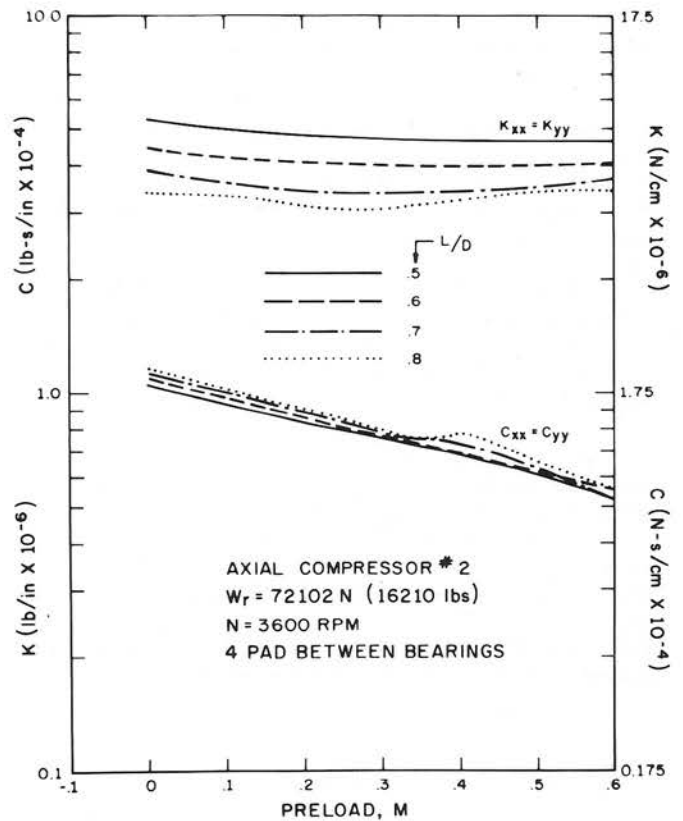


Figure 6. Variation in Stiffness and Damping with Preload and Length to Diameter Ratio, 4-Pad Bearing, $D = 20.32$ cm, 8.0 in.

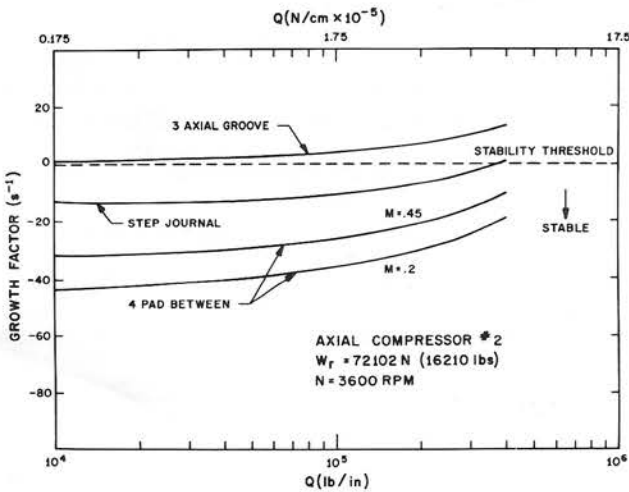


Figure 5. Stability Map, Axial Compressor Number 2.

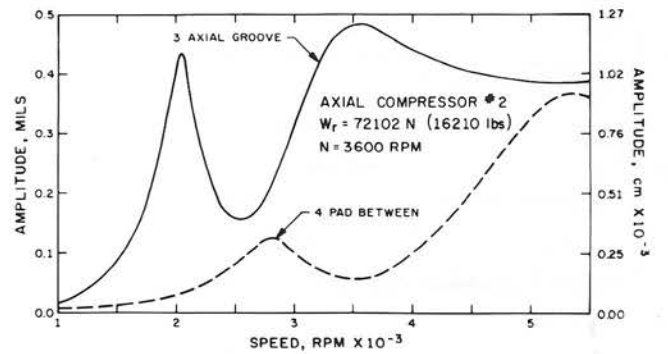


Figure 7. Relative Peak to Peak Response, Probe Location, Axial Compressor Number 2, 3-Axial Groove and 4-Pad Bearings.

large bearing loads becomes important and the largest pad length possible is also advantageous from this viewpoint.

Theoretical response plots for the compressor supported by 3-axial groove and 4-pad tilting pad bearings are shown in Figure 7. The curves are for the discharge end probe location and the response is relative to the support. About $4 W_r/N$ ounce-inches of unbalance is used to excite the compressor. The 4-pad bearing is extremely effective in reducing the synchronous vibration level at operating speed and in fact over the entire speed range shown.

The 3-axial groove response shows 2 peaks at around 2,000 RPM and 3,500 RPM. Close examination of the mode shapes and the machine critical speed map indicates that both peak responses are first mode excitations due to the asymmetry in the 3-axial groove bearings. The 4-pad tilt pad bearing with between pad loading is symmetric and results in only one peak in the operating range at 2800 RPM.

Vibration Analysis,
Axial Compressor Number 3

Machine number 3 weighs 31,661 N (7,118 lbs.) and has a

journal diameter of 16.51 cm (6.5 in.). Figure 8 is a stability plot for this compressor. The stability analysis predicts that the compressor may operate unstably with the standard 3-axial groove bearings. The step bearing design, however, places the compressor well within the stable region. Three different types of tilting pad designs are also considered: 4 pads with load between pads and 5 pads with load on and between pads. All tilt pad designs provide a large stability margin (growth factor between -50 and -60 for $Q = 1.75 \times 10^4$ N/cm, 10^4 lbs/in.). The 5-pad between is slightly superior to the 5-pad on. The 4-pad between design provides a slightly larger stability margin for low values of Q but becomes less stable for larger Q values compared to the 5-pad designs. This is probably due to the lack of stiffness asymmetry with the 4-pad between bearing and since the bearing is symmetric, $K_{xx} = K_{yy}$. Stiffness asymmetry is favorable to machine stability [5, 6, 7].

Figure 9 compares the theoretical response curves for the compressor supported by the 3-axial groove, the step journal and the 4-pad between bearing design. The response, relative to the support, is for the bearing centerline location with approximately $4 W_r/N$ ounce-inches of unbalance. Figure 10 illustrates the absolute response at the compressor's center. Note that for the fixed lobe designs, a peak response is predicted to be around 5,000 RPM, very close to the operating speed of 5,500 RPM. Another peak response is seen at around

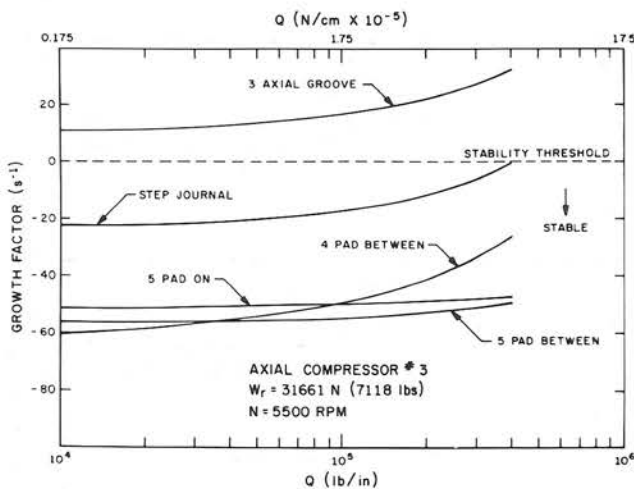


Figure 8. Stability Map, Axial Compressor Number 3.

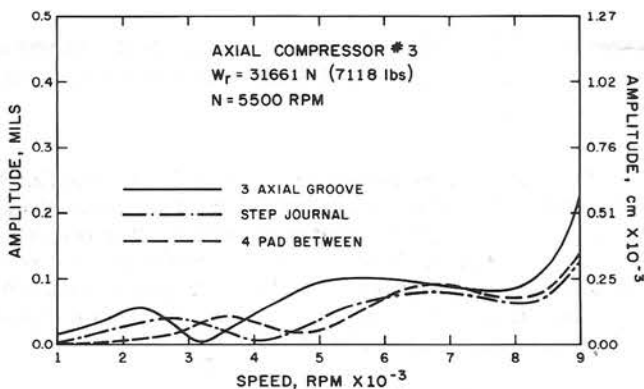


Figure 9. Relative Peak to Peak Response, Bearing Centerline, Axial Compressor Number 3, 3-Axial Groove, Step Journal and 4-Pad Bearings.

2,500 RPM. Again, the 4-pad bearing is effective in removing the peak response out of the operating range. Additionally, the sensitivity of the compressor is reduced with the 4-pad design over the fixed lobe cases.

All tilt pad designs are compared to the 3-axial groove bearing for machine number 3 in Figure 11. The 5-pad designs increase the compressor's sensitivity at the unbalance criticals over the 3-axial groove case. The 5-pad on bearing, being asymmetric, shows a slight bump at around 3,000 RPM as well as a larger peak at 4,200 RPM. In fact, this 4,200 RPM critical has the largest amplification of all bearing designs considered. The 5-pad between bearing shows only one peak response in the operating range since it is only slightly asymmetric. However, its peak is larger than the 4-pad between case.

Fixed Lobe Bearing Stability Analysis

A summary of the stability and speed parameters obtained from a bearing analysis for the fixed lobe bearings is listed in Table 3. The dimensionless speed parameter, $\bar{\omega}$, is defined as

$$\bar{\omega} = \omega \sqrt{\frac{mc}{W}} \quad (1)$$

where:

- ω = journal rotational speed (T^{-1})
- m = journal mass at bearing (FT^2L^{-1})
- W = bearing load (F)
- c = bearing radial clearance (L)

For horizontal machines with gravity loading only, equation (1) reduces to

$$\bar{\omega} = \omega \sqrt{c/g} \quad (2)$$

where g is the gravitational constant (LT^{-2}). Additional details may be found in Appendix 1 and reference [9].

From the bearing analysis, stability threshold speed parameters may be calculated. These parameters, $\bar{\omega}_{tr}$ and $\bar{\omega}_{tf}$ are functions of the bearing's stiffness and damping properties at a specific speed and the journal mass at the bearing (see Appendix 1). The quantity $\bar{\omega}_{tr}$ is the dimensionless threshold speed above which the journal would operate unstably assuming a rigid shaft. Shaft flexibility effects may be taken into account by adjusting $\bar{\omega}_{tr}$ as indicated in Appendix 1. The resulting parameter, $\bar{\omega}_{tf}$ includes the approximate effects of shaft flexibility on bearing stability. For example, from Table 3, compressor number 1 operating on 3-axial groove bearings has a dimen-

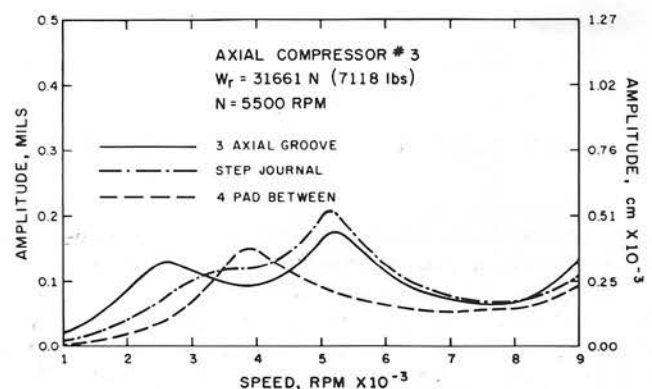


Figure 10. Absolute Peak to Peak Response, Compressor Center, Axial Compressor Number 3, 3-Axial Groove, Step Journal and 4-Pad Bearings.

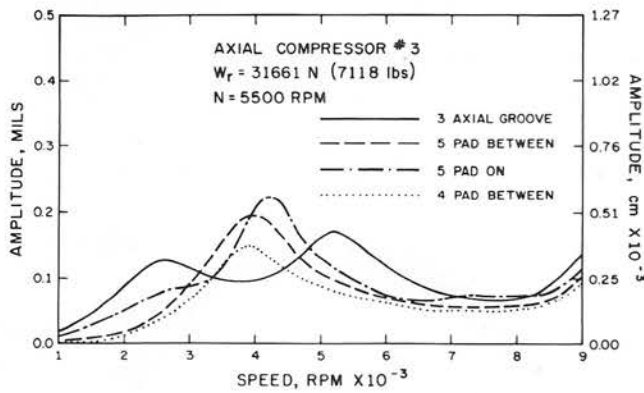


Figure 11. Absolute Peak to Peak Response, Compressor Center, Axial Compressor Number 3, 3-Axial Groove, 4- and 5-Pad Bearings.

sionless operating speed of $\bar{\omega} = 1.6$ ($N = 5,500$ RPM). Also, $\bar{\omega}_{tr} = 1.9$, which means that the axial compressor is operating below the rigid shaft threshold speed. However, $\bar{\omega}_{tf} = 1.4$ and the axial is predicted to operate above the stability threshold when shaft flexibility effects are considered. These threshold speed parameters are dimensionalized and indicated in Table 3 as N_{tr} and N_{tf} .

For all three machines, the bearing stability analysis predicts that the compressor is operating above the threshold speed on 3-axial groove bearings ($N > N_{tr}$). However, the step journal bearings have flexible shaft threshold speeds above operating speed ($N < N_{tr}$). These results also correspond to the full machine stability analyses from Figures 2, 5, and 8. A growth factor column is indicated on Table 3 for comparison. For all cases, when $N > N_{tr}$, the growth factor is positive indicating possible unstable operation. Additionally, when $N < N_{tr}$, the growth factor is negative indicating stable operation. Thus, for this type of turbomachinery, it appears that a bearing stability analysis including shaft flexibility effects is a good indicator of the stability characteristics of the machine.

In all three cases, the step journal bearing design is analytically effective in improving the compressor's stability characteristics over the 3-axial groove bearing. Reference [9] concludes that the optimum Sommerfeld number range for designing step bearings for improved stability characteristics is $S > 2.0$. However, step bearings are effective for the moderate range of Sommerfeld numbers ($0.1 \leq S \leq 1.0$) if the effects of shaft flexibility are small. The 3-axial compressors considered here fall into this category. As shaft flexibility increases, all fixed lobe bearings approach the stability characteristics of a

plain journal bearing. The large increase in rigid shaft stability performance for step bearings shown in Figure 12 for high Sommerfeld numbers may be misleading for machines with relatively flexible shafts. Conversely, the apparent small increase in stability for moderate Sommerfeld numbers may be a true indication of the actual increase in stability performance for relatively rigid shaft machines.

Axial Compressor Summary

Test stand and field experience has shown that these axial compressors usually run without any subsynchronous vibration with 3-axial groove bearings. Since the insert is manufactured either line-to-line or .051 mm (2.0 mils) tight in the shell, it is reasonable to expect the insert to be crushed. Crushing the insert results in a slight out of roundness or ellipticity. This ellipticity may increase the bearing's stability threshold speed. Furthermore, each pad or lobe may be slightly preloaded and offset [1]. This effect may also increase the stability threshold. However, some axials do exhibit a small subsynchronous component at certain stator settings.

TILTING PAD JOURNAL BEARING DESIGNS FOR HIGH SPEED CENTRIFUGAL COMPRESSORS

Stability Analysis, 8-Stage Centrifugal

In this section, a stability analysis is presented for a light

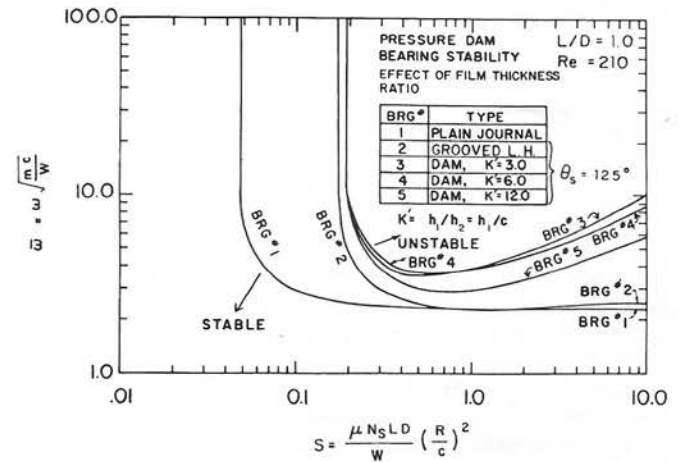


Figure 12. Step Bearing Stability Comparison with Plain Journal and Grooved Lower Half Bearings [9].

TABLE 3. SUMMARY OF FIXED LOBE BEARING STABILITY PARAMETERS AND THRESHOLD SPEEDS FOR THE THREE AXIAL COMPRESSORS.

Machine Number	Bearing Type	c		$\bar{\omega}^*$	$\bar{\omega}_{tr}^*$	$\bar{\omega}_{tf}^*$	N	N_{tr}^*	N_{tf}^*	Growth Factor ⁺
		(mils)	(mm)							
1	3-Axial Groove	3.0	.0762	1.6	1.9	1.4	5500	6510	4980	+ 4
1	Step Journal	3.0	.0762	1.6	2.9	2.2	5500	9960	7620	-22
2	3-Axial Groove	5.5	.1397	1.4	1.6	1.3	3600	4050	3380	+ 1
2	Step Journal	5.5	.1397	1.4	2.5	2.1	3600	6310	5280	-14
3	3-Axial Groove	4.5	.1143	2.0	2.0	1.7	5500	5600	4870	+11
3	Step Journal	4.5	.1143	2.0	3.2	2.8	5500	8930	7780	-22

* At Operating Speed
 +At $Q = 1.75 \times 10^4$ N/cm, 10^4 lbs/in (See Figures 2, 5 and 8)

($W_r = 2,986 \text{ N}$, 671 lbs.) high speed ($N = 13,500 \text{ RPM}$) 8-stage centrifugal compressor. The analysis includes the effects of 2 high pressure floating oil ring seals [10]. All other destabilizing effects such as internal friction due to shrink fits, labyrinth seal pressure pulsations and aerodynamic excitations are lumped into one parameter, aerodynamic cross-coupling.

From the critical speed and forced response analysis, the first rigid bearing critical is $N_{cr} = 4,700 \text{ RPM}$ and the first peak response speed is $N_1 = 4,500 \text{ RPM}$. The ratio of operating speed to N_{cr} is $\bar{N} = 2.9$.

The compressor is supported by 5-pad tilting pad bearings (Figure 13) load on pad, with a bearing radial clearance of $c_b = .0635 \text{ mm}$ (2.5 mils) and preload of $M = .45$ (c_b and M approximately nominal values). The bearing stiffnesses at operating speed are $K_{xx} = 740,250 \text{ N/cm}$ (423,000 lbs/in.) and $K_{yy} = 927,500 \text{ N/cm}$ (530,000 lbs/in.). The shaft stiffness is approximately $K_s = 369,250 \text{ N/cm}$ (211,000 lbs/in.) which results in a stiffness ratio of $\bar{K} = 4.5$ where

$$\bar{K} = \frac{K_{xx} + K_{yy}}{K_s} \quad (3)$$

The shaft stiffness may be approximated from

$$K_s = m_m \omega_{cr}^2 \quad (\text{FL}^{-1}) \quad (4)$$

where m_m is the approximate modal mass.

$$m_m = \frac{W_r}{2g} \quad (\text{FT}^2\text{L}^{-1}) \quad (5)$$

W_r = total rotor weight (F)

g = gravitational constant (LT^{-2})

$$\omega_{cr} = \frac{\pi}{30} N_{cr} \quad (\text{T}^{-1})$$

From Table 1, the stiffness ratios for the axial compressors range from $\bar{K} = .68$ to 2.3. It is clear that the centrifugal compressor's shaft is more flexible compared to the bearing stiffness than the three axial compressors considered in the previous section. Furthermore, the larger the stiffness ratio, the more sensitive the machine is to destabilizing forces [6]. Also from Table 1, the axial machines operate below N_{cr} whereas the centrifugal machine operates 2.9 times above N_{cr} , again making the centrifugal compressor much more susceptible to destabilizing excitation. Finally, the high pressure oil seals in conjunction with the high speed ratio of $\bar{N} = 2.9$ makes the centrifugal compressor sensitive to seal induced instability [10].

Considering all of these factors, it seems unlikely that any fixed lobe bearing design would permit the centrifugal compressor to operate below the stability threshold. In fact, in some cases it may be extremely difficult to design tilt pad bearings that insure stable operation for this class of compressor. The objective of the analysis presented in this section is to attempt to optimize the 5-pad tilt pad bearing design for favorable compressor's stability characteristics.

The stiffness and damping coefficients are shown in Figure 14 for the 5-pad tilting pad bearing with on pad loading and for the nominal bearing radial clearance value of $c_b = .0635 \text{ mm}$ (2.5 mils). The characteristics are plotted as a function of preload. The tolerance range on the preload is indicated ($.33 \leq M \leq .6$). Below $M = .18$, the top pads become unloaded and no longer contribute to bearing damping. This results in the

- R_v = RADIUS TO PIVOT
- R_p = PAD RADIUS OF CURVATURE
- $R_v = R_p$ WHEN $M = 0.0$

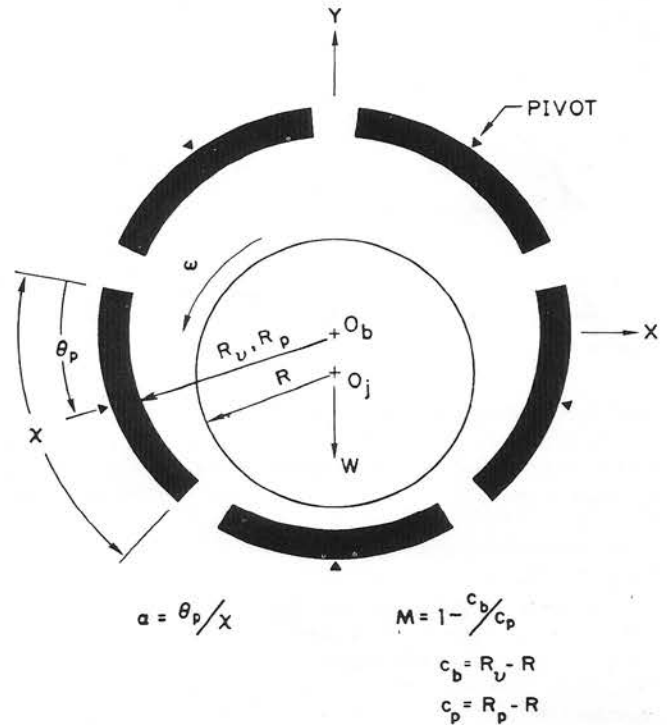


Figure 13. Five-Pad Tilting Pad Bearing.

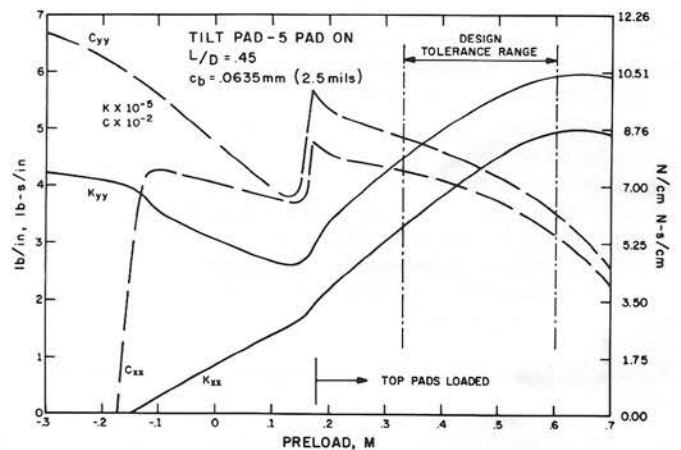


Figure 14. Variation in Stiffness and Damping with Preload, 5-Pad Bearing, $D = 9.21 \text{ cm}$, 3.625 in, 8 Stage Centrifugal.

abrupt decrease in damping below a preload of .18. As preload further decreases into the negative region, the horizontal stiffness and damping rapidly approach zero below $M = -.1$.

A stability map for the centrifugal compressor is shown in Figure 15 as a function of bearing preload. For the design seal inlet pressure, the compressor is predicted to operate either unstably or on the stability threshold, depending on the amount of destabilizing excitation, Q . Within the tolerance range for the tilt pad bearing clearance and preload, the stability analysis predicts a real root of +18 for $Q = 1751 \text{ N/cm}$ (1000

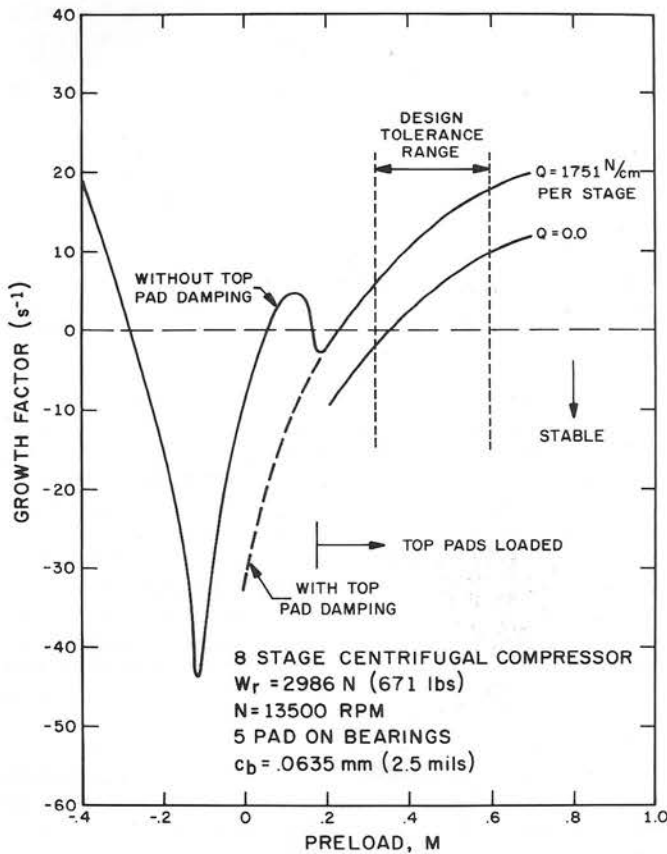


Figure 15. Variation in Stability Performance with 5-Pad Bearing Preload, 8-Stage Centrifugal Compressor.

lbs/in.) per stage for $M = .6$ (+6.5 for $M = .33$). If preload is decreased outside the tolerance range, stability improves until the top pads become unloaded and top pad damping is neglected. Since there is an abrupt decrease in damping, stability deteriorates as preload decreases from .18 to .12. Further decreasing preload enhances the compressor's stability characteristics rapidly until $M = -.12$. At this point, the negative preload causes the horizontal damping to decrease sharply and stability again deteriorates.

The dangers of negative preload become clear from Figures 14 and 15. Although a slight negative preload is tolerable and indeed beneficial, preloads that range below $M = -.1$ may cause severe stability problems. Often, tilt pad bearings are designed for a nominal preload of zero. Care must be taken to insure that the tolerance range does not include preloads below $M = -.1$. Thermal and load distortions may also contribute to decreasing a pad's preload. A good indication of this type of problem is evidence of rubbing at the pads leading and/or trailing edges.

Tilt Pad Stability Optimization, 8-Stage Centrifugal Compressor

Since Figure 15 indicates that the compressor may operate on the stability threshold at bearing and seal design conditions, it may be possible to improve the centrifugal compressor's stability characteristics by redesigning the tilt pad bearings. The obvious intent is to increase bearing damping without a corresponding increase in bearing stiffness. In the previous section, this was accomplished by increasing the pad length for the axial compressor's 4-pad tilt pad bearings. Table 4 summarizes the

effect of changing pad length on the stiffness and damping properties of the centrifugal compressor's 5-pad bearings. As the length to diameter ratio increases from the $L/D = .45$ design value, both stiffness and damping increase. This is a characteristic of heavily preloaded tilt pad bearings in the high Sommerfeld number range above $S = 1.0$ [11]. Table 4 indicates that the 5-pad bearing's Sommerfeld number ranges from 2.1 for an L/D of .33 to $S = 6.2$ for $L/D = 1.0$.

The stiffness ratio, \bar{K} , is also indicated on Table 4. Since bearing stiffness increases as L/D increases, \bar{K} increases. Even though damping also increases, the increase in stiffness ratio permits less bearing damping to be transmitted to the compressor center as effective damping to combat the destabilizing forces. As \bar{K} increases, the compressor's first mode shape looks more and more like a flexible shaft bending mode with the bearings as nodal points. In this configuration with a high K value, only a small percentage of bearing damping is active in stabilizing the compressor [6].

Decreasing the L/D ratio is also considered. Table 4 shows that as L/D decreases from .45 to .33, \bar{K} decreases. However, since damping also decreases, no clear advantage is obtained from reducing pad length.

Another possibility to increase damping is to increase the pad arc length, χ . The design value is $\chi = 56^\circ$. Figure 16 illustrates the effects of increasing the arc length to $\chi = 65^\circ$. Damping does indeed increase but so does stiffness, providing the same effects as increasing the pad length. Again, no clear advantage is obtained.

Figure 14 shows that damping may be increased and stiffness decreased if the preload is reduced below the design tolerance range. For lower preloads, Figure 15 exhibits improved stability characteristics for the centrifugal compressor. A preload range between 0.0 and 0.3 would seem preferable to the design range of 0.33 to 0.60. This may be accomplished by reducing the pad's radius of curvature, R_p . The shaft diameter is

$$D = 9.2075^{+.0000}_{-.0013} \text{ cm}$$

$$D = 3.6250^{+.0000}_{-.0005} \text{ in.}$$

At present design conditions, the pad bore diameter, $D_p = 2R_p$ is

$$D_p = 9.2304^{+.0013}_{-.0000} \text{ cm}$$

$$D_p = 3.6340^{+.0005}_{-.0000} \text{ in.}$$

This results in a pad radial clearance range of $c_p = .114$ to .127 mm (4.5 to 5.0 mils). With a .0127 mm (0.5 mil) tolerance on the housing diameter and pad thickness, the design tolerance range on the bearing radial clearance is $c_b = .051$ to .076 mm (2.0 to 3.0 mils). The present design is indicated as design number 1 in Table 5. Reducing the bore diameter by .0254 mm (1.0 mils) while keeping c_b constant results in a preload range of $M = .25$ to .56. A .0762 mm (3.0 mils) reduction in D_p gives a 0.0 to .43 range on preload. Further reducing D_p places preload in the negative region (design number 5).

Design numbers 6 through 10 in Table 5 show the effect on preload tolerance range for a larger bearing clearance of .064 to .089 mm (2.5 to 3.5). Design number 8 results in a preload range of 0.0 to .38. A further reduction in c_b is indicated in design numbers 11 through 14. The preload ranges between 0.0 and .33 for design number 12.

TABLE 4. STIFFNESS AND DAMPING PROPERTIES AS A FUNCTION OF PAD LENGTH FOR THE 8-STAGE CENTRIFUGAL COMPRESSORS 5-PAD TILTING PAD BEARINGS, LOAD ON PAD, $M = .45$, $\chi = 56^\circ$, $N = 13,500$ RPM.

L/D*	S ⁺	K _{xx} × 10 ⁻⁶		K _{yy} × 10 ⁻⁶		\bar{K}	C _{xx}		C _{yy}	
		lb/in	N/cm	lb/in	N/cm		lb-s/in	N-s/cm	lb-s/in	N-s/cm
.33	2.1	.266	.466	.464	.813	3.5	222	389	301	527
.45 [‡]	2.8	.423	.741	.530	.928	4.5	392	686	440	771
.70	4.4	.803	1.41	.849	1.49	7.8	823	1441	838	1467
1.0	6.2	1.24	2.17	1.32	2.31	12.1	1520	2662	1790	3135

* D = 9.21 cm (3.625 in) constant
 + Based on $c_b = .0635$ mm (2.5 mils)
 ‡ Design Conditions

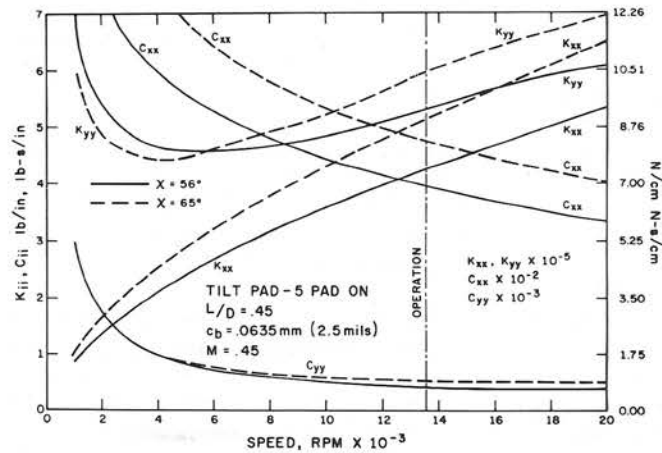


Figure 16. Variation in Stiffness and Damping with Pad Arc Length and Speed, $D = 9.21$ cm, 3.625 in, 8-Stage Centrifugal Compressor.

While the 0.0 to .43 range on preload for design number 4 is close to the desired range of 0.0 to .33, a partial overlap exists with the present design tolerance range of .33 to .6. This indicates that even though the nominal preload value is lower, there is no guarantee that design number 4 will produce a lower preload and improved stability characteristics. Bearing design number 8 is somewhat better with only a slight overlap. The desired tolerance range is realized with design number 12. However, this design has a large bearing radial clearance of .089 mm (3.5 mils) nominal. It is preferable to maintain the tilt pad bearing clearance at 1 mil radial clearance per inch of shaft radius plus 1 mil. This clearance should provide a substantial amount of damping to the turborotor system. This results in a radial clearance of $c_b = 0.714$ mm (2.8125 mils) which is very close to the nominal value of design number 8. As c_b increases from this value, the amount of damping supplied by the bearing decreases. Thus a possible compromise redesign is design number 8 with the preload range of 0.0 to .38.

An interesting trend from Table 5 is that preload range increases as the nominal preload decreases. For example, design number 1 has a nominal preload of .465 and a range of .27. The nominal preload for design number 4 is .215 with a range of .43. Also, the smaller the journal diameter, the larger the preload range since the tolerances on the journal diameter, pad thickness, housing diameter and bore diameter remain the

TABLE 5. CLEARANCE TOLERANCES AND PRELOAD RANGE FOR THE 8-STAGE CENTRIFUGAL COMPRESSORS 5-PAD TILTING PAD BEARINGS, LOAD ON PAD, $\chi = 56^\circ$, $L/D = .45$.

Bearing Design No.	c_b (radial)				c_p (radial)				M		Bore Dia.	
	mils		mm		mils		mm		min	max	in	cm
	min	max	min	max	min	max	min	max				
1*	2.0	3.0	.051	.076	4.5	5.0	.114	.127	.33	.60	3.634	9.230
2	2.0	3.0	.051	.076	4.0	4.5	.102	.114	.25	.56	3.633	9.228
3	2.0	3.0	.051	.076	3.5	4.0	.089	.102	.14	.50	3.632	9.225
4	2.0	3.0	.051	.076	3.0	3.5	.076	.089	0.0	.43	3.631	9.223
5	2.0	3.0	.051	.076	2.5	3.0	.064	.076	-.20	.33	3.630	9.220
6	2.5	3.5	.064	.089	4.5	5.0	.114	.127	.22	.50	3.634	9.230
7	2.5	3.5	.064	.089	4.0	4.5	.102	.114	.13	.44	3.633	9.228
8	2.5	3.5	.064	.089	3.5	4.0	.089	.102	0.0	.38	3.632	9.225
9	2.5	3.5	.064	.089	3.0	3.5	.076	.089	-.17	.29	3.631	9.223
10	2.5	3.5	.064	.089	2.5	3.0	.064	.076	-.40	.17	3.630	9.220
11	3.0	4.0	.076	.102	4.5	5.0	.114	.127	.11	.40	3.634	9.230
12	3.0	4.0	.076	.102	4.0	4.5	.102	.114	0.0	.33	3.633	9.228
13	3.0	4.0	.076	.102	3.5	4.0	.089	.102	-.14	.25	3.632	9.225
14	3.0	4.0	.076	.102	3.0	3.5	.076	.089	-.33	.14	3.631	9.223

*Design Conditions

same at .0127 mm(.5 mils). Conversely, the larger the journal diameter, the tighter the preload range. For example, for axial compressor number 2 with a shaft diameter of 20.32 cm (8.0 in.) and a nominal preload of .5, the preload range is .15 (.42 to .57). Additionally, the smaller the shaft diameter, the more sensitive the tilt pad bearing would be to thermal and load effects on preload.

With all of the above considerations in mind, it is extremely difficult to recommend a design change in the tilt pad bearings that may offer a clear improvement in the compressor's stability characteristics. The analysis predicts that the centrifugal compressor will operate free of subsynchronous vibration since the level of aerodynamic excitation will be small. The machine is used to compress hydrogen which has an extremely low molecular weight and the discharge pressure is only 76 N/cm² (110 psi). Both of these facts point to low aerodynamic excitation. In contrast, the Kaybob compressor [12] has a discharge pressure of around 1100 to 1378 N/cm² (1600 to 2000 psi) and compresses well gas which has a considerably higher mole weight than hydrogen.

The centrifugal compressor analyzed in this section ran successfully on the test stand at full speed and full pressure without any subsynchronous vibration. Helium was used as the test gas.

Tilt Pad Stability Optimization, 2-Stage Centrifugal

To further illustrate some of the design concepts discussed in the previous section, a stability optimization study is presented here for a 2-stage centrifugal compressor. The total rotor weight is 712 N (160 lbs.) and the operating speed is 12,500 RPM. Five-pad bearings support the compressor with on pad loading and a journal diameter of 6.985 cm (2.75 in.). The optimization includes the effects of 2 high pressure oil seals.

Non-dimensional curves are shown in Figure 17 [6, 11] for the compressor's 5-pad bearings. Two preload values of

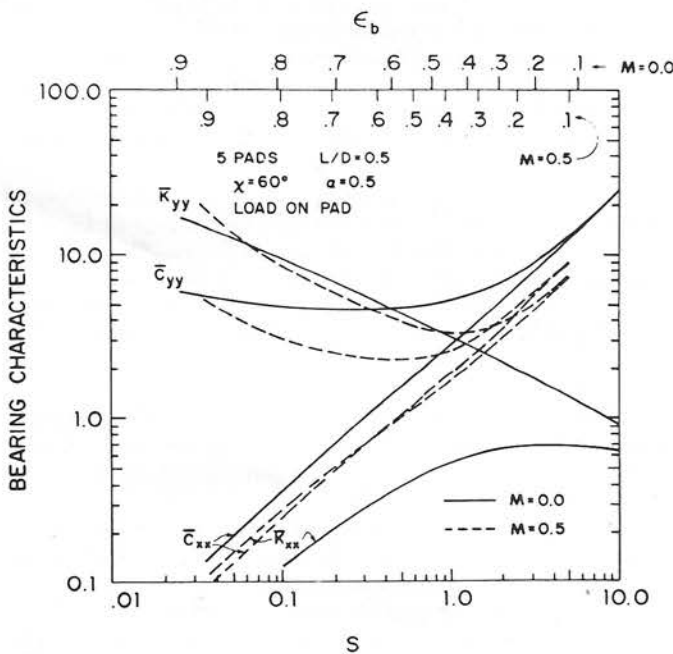


Figure 17. Nondimensional 5-Pad Bearing Characteristics, 8-Stage Centrifugal Compressor [6, 11].

M = 0.0 and 0.5 are indicated. For this centrifugal compressor and many other high speed, lightweight rotors, the Sommerfeld number ranges from 1.0 and above. For a given Sommerfeld number in this range (given bearing clearance, c_b), Figure 17 shows that decreasing preload decreases stiffness and increases damping. Both of these effects which are also evident in Figure 14, are helpful in improving stability performance (Figure 15). This condition provides an extremely useful guideline to tilt pad bearing design.

The effect of pad and bearing clearance on the stability characteristics of the 2-stage compressor is illustrated in Figure 18 where preload is plotted against growth factor. The solid line curve is for a constant pad clearance of c_p = .1201 mm (4.73 mils) and represents the variance in stability as bearing clearance changes. The current bearing design is indicated between a preload of .55 to .7. Decreasing preload below the design tolerance range by increasing c_b, improves stability until preload drops below M = .4. As preload decreases below .4, stability deteriorates even though the stiffness ratio, K-bar, decreases. One reason for this is the decrease in bearing damping as c_b increases above the mil per inch plus one standard. This trend may be observed in Table 6 which lists the bearing characteristics for the curves of Figure 18. Note that the standard bearing clearance is .603 mm (2.375 mils) which results in a preload of M = .5. Optimum stability occurs at M = .4 and c_b = .0721 mm (2.84 mils).

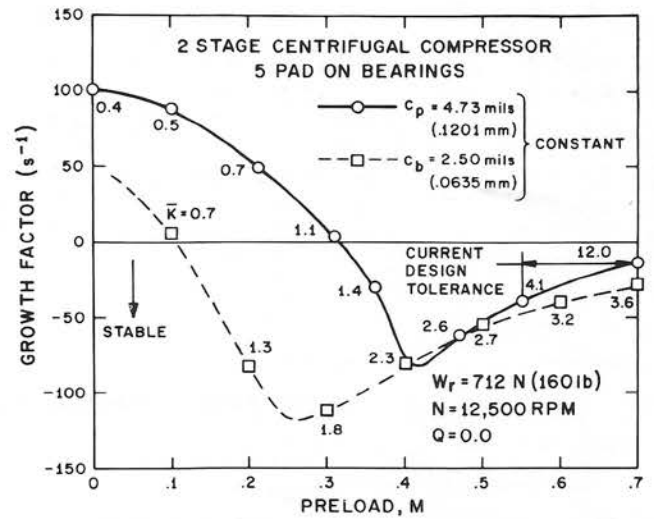


Figure 18. Variation in Stability Performance with Preload, Pad and Bearing Clearance, 2-Stage Centrifugal Compressor.

Choosing a bearing clearance of c_b = .0635 mm (2.5 mils), Figure 18 (dashed line) shows the change in stability as preload or pad clearance changes. Again stability improves as preload decreases down to M = .25. Below .25, stability starts to decrease even though stiffness ratio decreases. Table 6 indicates that damping continues to increase down to a preload of .2. This deterioration in stability is probably due to the dominance of the oil seals for low values of bearing stiffness. As the bearings become softer, the oil seal stiffness becomes predominant and the compressor essentially rides on the seals producing poor stability characteristics. From Figure 18, stiffness ratios of around K-bar = 1.0 and below are unacceptable for this compressor.

The redesigned optimized bearing ranges in bearing clearance from .0483 to .0673 mm (1.9 to 2.65 mils) and in preload from .52 to .24. Current and redesign bearing characteristics are also summarized in Table 6. Figure 19 is a stability

TABLE 6. FIVE-PAD BEARING CHARACTERISTICS AND STABILITY PERFORMANCE FOR THE 2-STAGE CENTRIFUGAL COMPRESSOR.

S	c_b		c_p		M	$K_{xx} \times 10^{-5}$		$K_{yy} \times 10^{-5}$		\bar{K}	C_{xx}		C_{yy}		Real Root Q=0.0	
	mils	mm $\times 10^{-2}$	mils	mm $\times 10^{-2}$		lbs/in	N/cm	lbs/in	N/cm		lb-s/in	N-s/cm	lb-s/in	N-s/cm		
	N = 12,500 RPM															
9.2	1.42	3.61	4.73	12.01	0.70	7.66	13.41	7.76	13.59	12.0	421	737	425	744	- 13	
4.1	2.13	5.41			0.55	2.59	4.54	2.72	4.76	4.1	211	369	217	380	- 39	
3.0	2.50	6.35			0.47	1.57	2.75	1.72	3.01	2.6	156	273	164	287	- 62	
2.1	3.00	7.62			0.36	0.84	1.47	1.02	1.79	1.4	110	193	121	212	- 30	
1.8	3.26	8.28			0.31	0.61	1.07	0.80	1.40	1.1	94	165	106	186	+ 3	
1.3	3.73	9.47			0.21	0.34	0.60	0.58	1.02	0.7	75	131	92	161	+ 48	
1.0	4.25	10.80			0.10	0.17	0.30	0.43	0.75	0.5	48	84	58	102	+ 89	
0.8	4.73	12.01			0.00	0.10	0.18	0.46	0.81	0.4	41	72	61	107	+100	
	3.0	2.50	6.35	12.50	31.75	0.80	2.48	4.34	2.57	4.50	3.9	95	166	97	170	- 20
				8.33	21.16	0.70	2.27	3.98	2.37	4.15	3.6	122	214	125	219	- 28
				6.25	15.88	0.60	1.98	3.47	2.10	3.68	3.2	139	243	144	252	- 39
				5.00	12.70	0.50	1.68	2.94	1.81	3.17	2.7	153	268	159	278	- 55
				4.17	10.59	0.40	1.37	2.40	1.52	2.66	2.3	164	287	173	303	- 81
				3.57	9.07	0.30	1.06	1.86	1.23	2.15	1.8	174	305	185	324	-113
				3.13	7.95	0.20	0.77	1.35	0.96	1.68	1.3	185	324	198	347	- 83
				2.78	7.06	0.10	0.42	0.74	0.44	0.77	0.7	152	266	118	207	+ 4
CURRENT	9.5	1.40	3.56	4.67	11.86	0.70	7.86	13.76	7.96	13.93	12.4	433	758	436	763	- 13 MIN
	5.9	1.78	4.52	4.81	12.22	0.63	4.31	7.54	4.43	7.75	6.8	291	509	295	516	- 28 NOM
	4.0	2.15	5.46	4.78	12.14	0.55	2.57	4.50	2.68	4.69	4.1	205	359	209	366	- 50 MAX
RE-DESIGN	5.2	1.90	4.83	3.95	10.03	0.52	3.14	5.50	3.27	5.72	5.0	277	485	283	495	- 52 MIN
	3.6	2.28	5.79	3.68	9.35	0.38	1.62	2.84	1.76	3.08	2.6	204	357	212	371	-127 NOM
	2.7	2.65	6.73	3.50	8.89	0.24	0.78	1.37	0.98	1.72	1.4	159	278	172	301	- 65 MAX

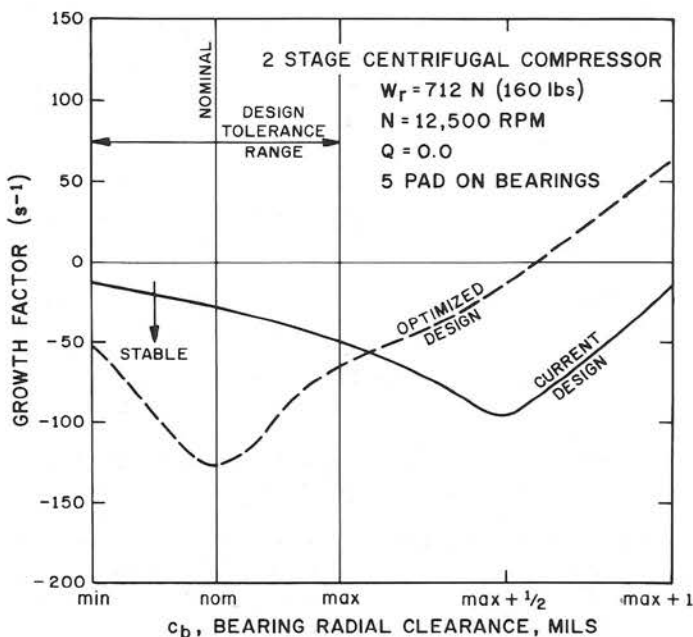


Figure 19. Stability Performance Over the 5-Pad Bearing Tolerance Range Plus 1 Mil Above Maximum, 2-Stage Centrifugal Compressor.

plot for the current and redesigned tilt pad bearings over the tolerance range on bearing clearance. Also shown are c_b values up to maximum plus 1.0 mils radial. Pivot and babbitt wear after long periods of operation may tend to increase c_b beyond the design tolerance range. The current design provides a stability optimum at maximum plus .5 mils while the redesigned bearing optimizes stability at nominal clearance.

The optimized design provides a substantial increase in stability at nominal bearing clearance with a growth factor of -127 compared to -28 for the current design. However, for bearing clearances above maximum plus .5 mils, the optimized bearing ranges into the unstable region. Since the optimized design is softer than the current design, the seal stiffness begins to dominate at a lower bearing clearance, thereby decreasing stability.

Figure 20 is a stability plot as a function of compressor speed for the optimized redesigned bearing, nominal clearance values. Stability is optimum at about 11,500 RPM with a growth factor of around -138.

Although the journal diameter is smaller than the 8-stage compressor of the last section, the tolerance range on clearance is tighter. For the 2-stage compressor with $D = 6.985$ cm (2.75 in.), the tolerance range on bearing radial clearance is .01905 mm (.75 mils) and .28 on preload (redesign bearing). The 8-stage compressor with $D = 9.21$ cm (3.625 in.) has a .0254 mm (1.0 mil) radial tolerance and .27 on preload (current design). The bearings for the 2-stage compressor are manufac-

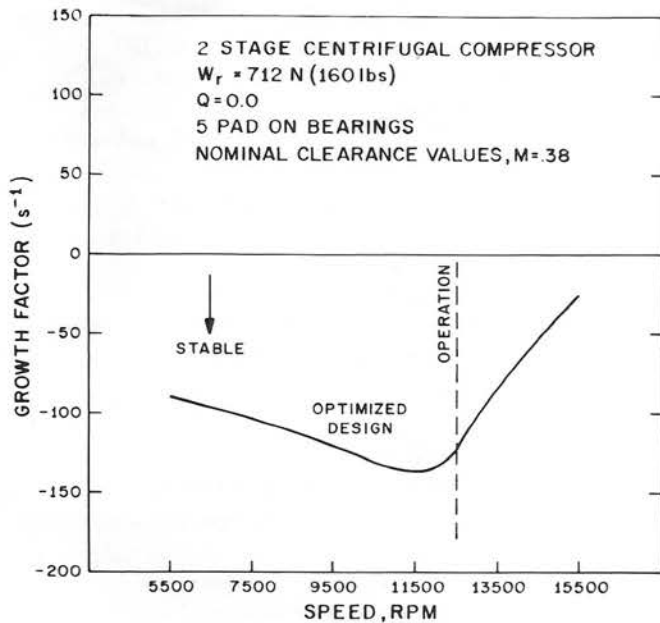


Figure 20. Stability with Speed, Optimized 5-Pad Design, 2-Stage Centrifugal Compressor.

tured with a tolerance on the pad thickness of $\pm .00254$ mm (± 0.1 mils) which results in a tighter clearance range.

SUMMARY AND CONCLUSIONS

The 3-axial groove inserts that support the axial compressors are often crushed in the bearing shell causing a slight ellipticity. This out of roundness along with each lobe possibly being preloaded or offset, results in stable compressor operation. However, clearances are usually kept on the tight side in order to enhance the bearing's stability characteristics.

Step journal bearings can successfully be designed for axial compressors even though the Sommerfeld number is in the moderate range (between 0.1 and 1.0). Since these machines operate well below the rigid bearing critical, the effect of shaft flexibility on the rigid rotor stability parameter is small. Therefore, the relative improvement in stability performance seen on a rigid rotor stability map is a true indication of the step bearings' ability to suppress oil whirl.

The 4-pad tilting pad bearing with between pivot loading is extremely effective in eliminating subsynchronous vibration. Also, due to its symmetric properties, the bearing is useful in moving peak response speeds out of the operating speed range. Overall synchronous response levels are lower compared to 3-axial groove and step journal bearings. Furthermore, response levels at resonance speeds are the lowest for the 4-pad bearing compared to all other designs considered (5-pad on and between, 3-axial groove and step journal).

Increasing the length to diameter ratio for the 4-pad between design provides increased damping with reduced stiffness. Therefore, in the moderate Sommerfeld number range, 4-pad bearings should be designed with the longest pad length possible.

The 5-pad bearings (on and between pad loading) also provide a wide stability margin for axial compressor number 3. Furthermore, being only slightly asymmetric, they are effective in eliminating the split critical speeds evident with 3-axial groove bearings. However, the resulting peak response vibration level is the largest compared to all other designs consid-

ered (4-pad between and 3-axial groove). This high response at the resonance speed for 5-pad bearings has also been observed experimentally in reference [14].

For turbomachinery whose weight and speed place them into the same class as axial compressors, a bearing stability analysis is effective in predicting the overall machine stability performance. Shaft flexibility effects can easily be incorporated into the rigid rotor stability parameter. When these effects are included, the threshold speed calculated from a bearing analysis accurately predicts the machine's stability margin compared to a full system stability analysis.

Some important tilt pad bearing design guidelines can be deduced from the results of the stability analyses for the 2 centrifugal compressors. Tilt pad bearing clearances should be maintained close to 1 mil per inch of journal radius plus 1 mil radial. This clearance should provide sufficient bearing damping to the rotor system. Opening up the bearing clearance results in large decreases in bearing damping and deterioration in stability performance.

Reducing preload by decreasing the pad clearance results in increase damping and decreased stiffness. Both of these effects are beneficial in providing good stability performance. As bearing stiffness is reduced, the stiffness ratio decreases thereby allowing more bearing damping to be effective in combating destabilizing excitations.

However, there are many potential problems with lightly preloaded bearings. First, if the top pads become unloaded, their contribution to bearing damping is eliminated. Also, unloaded pads may have a tendency to flutter. Furthermore, if the nominal preload is 0.0, negative preloads may result from the range on the clearance tolerances. This may be amplified during actual operation. Pivot and babbitt wear would tend to increase the bearing clearance and thus move the preload further into the negative region. Large negative preloads result in the loss of horizontal stiffness and damping. This effect is extremely detrimental to stability performance. Finally, bearings that are too soft may allow the machine to ride on the oil seals causing poor stability.

In the high Sommerfeld number range associated with high speed, light turbomachinery, increasing pad axial and/or arc length does not provide any clear cut advantage in stability. Any increase in bearing surface increases damping. However, stiffness also increases thereby allowing less bearing damping to be effective.

Consideration of the clearance tolerance range when designing tilt pad bearings is extremely important. The importance is magnified when the journal diameter is small since the tolerance range becomes larger. Often, a redesign on preload to improve stability may not guarantee any change due to overlapping tolerances ranges.

REFERENCES

1. Kirk, R. G., "The Influence of Manufacturing Tolerances on Multi-Lobe Bearing Performance in Turbomachinery," *Topics in Fluid Film Bearing and Rotor Bearing System Design and Optimization*, 1978 ASME Design Engineering Conference, April 1978, pp. 108-129.
2. Lund, J. W., "Stability and Damped Critical Speeds of a Flexible Rotor in Fluid-Film Bearings," *Journal of Engineering for Industry*, Trans. ASME, Vol. 96, No. 2, May 1974, pp. 509-517.
3. Gunter, E. J., "Rotor-Bearing Stability," *Proceedings of the First Turbomachinery Symposium*, Texas A&M Uni-

- versity, College Station, Texas, October 1972, pp. 119-141.
- Alford, J. S., "Protecting Turbomachinery from Self-Excited Rotor Whirl," *Journal of Engineering for Power*, Trans. ASME, No. 4, October 1965, pp. 333-344.
 - Warner, R. E. and Soler, A. I., "Stability of Rotor-Bearing Systems with Generalized Support Flexibility and Damping and Aerodynamic Cross-Coupling," *Journal of Lubrication Technology*, Trans. ASME, Vol. 97, No. 3, July 1975, pp. 461-471.
 - Nicholas, J. C., Gunter, E. J., and Barrett, L. E., "The Influence of Tilting Pad Bearing Characteristics on the Stability of High Speed Rotor-Bearing Systems," *Topics in Fluid Film Bearing and Rotor Bearing System Design and Optimization*, 1978 ASME Design Engineering Conference, April 1978, pp. 55-78.
 - Gunter, E. J. and Trumpler, P. R., "The Influence of Internal Friction on the Stability of High-Speed Rotors with Anisotropic Supports," *Journal of Engineering for Industry*, Trans. ASME, Vol. 91, No. 4, November 1969, pp. 1105-1113.
 - Black, H. F., "The Stabilizing Capacity of Bearings for Flexible Rotors with Hysteresis," *Journal of Engineering for Industry*, Trans. ASME, February 1976, pp. 87-91.
 - Nicholas, J. C. and Allaire, P. E., "Analysis of Step Journal Bearings-Finite Length, Stability," to be published in ASLE Trans., No. 78-LC-6B-2.
 - Kirk, R. G. and Miller, W. H., "The Influence of High Pressure Oil Seals on Turbo-Rotor Stability," ASLE Trans., Vol. 22, No. 1, January 1979, pp. 14-24.
 - Nicholas, J. C., Gunter, E. J., and Allaire, P. E., "Stiffness and Damping Coefficients for the Five-Pad Tilting-Pad Bearing," ASLE Trans., Vol. 22, No. 2, April 1979, pp. 113-124.
 - Smith, K. J., "An Operation History of Fractional Frequency Whirl," *Proceedings of the Fourth Turbomachinery Symposium*, Texas A&M University, College Station, Texas, 1975, pp. 115-125.
 - Allaire, P. E., "Design of Journal Bearings for High Speed Rotating Machinery," *Fundamentals of the Design of Fluid Film Bearings*, an ASME publication, 1979, pp. 45-84.
 - Leader, M. E., Flack, R. D., and Allaire, P. E., "Experimental Study of Three Journal Bearings with a Flexible Rotor," ASLE Preprint No. 79-AM-6D-2, May 1979.

NOMENCLATURE

- | | | | |
|--|--|--|---|
| c | = bearing radial clearance (L) | h_1, h_2 | = step journal bearing pocket clearance, bearing clearance ($h_2 = c$) (L) |
| c_b | = $R_v - R$, tilt pad bearing assembled radial clearance in line with a pivot (L) | $K_{xx}, K_{xy}, K_{yx}, K_{yy}$ | = bearing stiffness coefficients (FL^{-1}) |
| c_p | = $R_p - R$, pad radial clearance (L) | $\bar{K}_{xx}, \bar{K}_{xy}, \bar{K}_{yx}, \bar{K}_{yy}$ | = dimensionless stiffness coefficients, $\bar{K}_{ij} = K_{ij}(c/W)$, ($c = c_b$, tilt pad bearings) |
| $C_{xx}, C_{xy}, C_{yx}, C_{yy}$ | = bearing damping coefficients (FTL^{-1}) | \bar{K} | = $(K_{xx} + K_{yy})/K_s$, stiffness ratio |
| $\bar{C}_{xx}, \bar{C}_{xy}, \bar{C}_{yx}, \bar{C}_{yy}$ | = dimensionless damping coefficients, $\bar{C}_{ij} = C_{ij}(wc/W)$, ($c = c_b$, tilt pad bearings) | K_s | = $m_m \omega_{cr}^2$, shaft stiffness, (FL^{-1}) |
| D | = $2R$, journal diameter (L) | K' | = $h_1/h_2 = h_1/c$, step journal bearing film thickness ratio |
| D_p | = $2R_p$, pad bore diameter, tilt pad bearings (L) | L | = bearing axial length (L) |
| \bar{D} | = $\Omega \sqrt{M'}$ (T^{-1}) | L_b | = bearing span (L) |
| e_b | = bearing eccentricity (L) | M | = $1 - (c_b/c_p)$, tilt pad bearing preload |
| g | = gravitational acceleration constant (LT^{-2}) | M' | = $mc\omega^2/W$ |
| | | m | = journal mass (FT^2L^{-1}) |
| | | m_m | = modal mass (FT^2L^{-1}) |
| | | N, N_s | = shaft rotational speed (RPM), (RPS) |
| | | N_{tr} | = rigid rotor stability threshold speed (RPM) |
| | | N_{tf} | = stability threshold speed including shaft flexibility effects (RPM) |
| | | N_{cr} | = first rigid bearing critical speed (RPM) |
| | | \bar{N} | = N/N_{cr} , operating speed ratio |
| | | O_b, O_j | = bearing and journal centers |
| | | Q | = aerodynamic cross coupling (FL^{-1}) |
| | | R | = journal radius (L) |
| | | R_v | = radius from bearing center to pivot, tilt pad bearings (L) |
| | | R_p | = pad radius of curvature (L) |
| | | R_e | = $\frac{\rho V_c}{\mu}$, bearing Reynolds number |
| | | S | = $\frac{\mu N_s L D}{W} \left(\frac{R}{c}\right)^2$, Sommerfeld number ($c = c_b$, tilt pad bearings) |
| | | V | = $R\omega$, velocity of journal (LT^{-1}) |
| | | W | = bearing external load (F) |
| | | W_r | = total rotor weight (F) |
| | | X, Y | = coordinate system for rotating journal in bearing housing |
| | | \bar{X}, \bar{Y} | = $X/c, Y/c$ |
| | | $\dot{\bar{X}}, \dot{\bar{Y}}$ | = $d\bar{X}/d(\omega t), d\bar{Y}/d(\omega t)$ |
| | | $\ddot{\bar{X}}, \ddot{\bar{Y}}$ | = $d^2\bar{X}/d(\omega t)^2, d^2\bar{Y}/d(\omega t)^2$ |
| | | α | = θ_p/χ , bearing offset factor |
| | | ϵ_b | = e/c_b , eccentricity ratio |
| | | θ_p | = angle from leading edge of pad to pad pivot point (degrees) |
| | | θ_s | = location of step measured with rotation from positive X-axis (degrees) |
| | | μ | = average fluid viscosity (FTL^{-2}) |
| | | ρ | = fluid density (FT^2L^{-4}) |
| | | χ | = pad arc length (degrees) |
| | | ω, ω_{cr} | = shaft rotational speed, first rigid bearing critical speed (T^{-1}) |
| | | $\bar{\omega}$ | = $\omega \sqrt{\frac{mc}{W}}$, dimensionless speed parameter |
| | | $\bar{\omega}_{tr}$ | = dimensionless rigid rotor stability threshold speed |

$\bar{\omega}_{tr}$ = dimensionless stability threshold speed with shaft flexibility effects
 Ω = journal whirl speed (T^{-1})

APPENDIX

DERIVATION OF RIGID ROTOR STABILITY THRESHOLD SPEED

The rigid rotor stability threshold speed parameter, $\bar{\omega}_{tr}$, is derived in reference [9]. The derivation is included here for convenience and clarity.

Bearing stiffness and damping coefficients provide a means of investigating the stability of the journal about the bearing-journal equilibrium position. The linearized equations of motion in non-dimensional form are

$$\ddot{\bar{X}} + \frac{W}{mc\omega^2} \left[\bar{C}_{xx}\dot{\bar{X}} + C_{xy}\dot{\bar{Y}} + \bar{K}_{xx}\bar{X} + \bar{K}_{xy}\bar{Y} \right] = 0 \quad (A-1)$$

$$\ddot{\bar{Y}} + \frac{W}{mc\omega^2} \left[\bar{C}_{yx}\dot{\bar{X}} + C_{yy}\dot{\bar{Y}} + \bar{K}_{yx}\bar{X} + \bar{K}_{yy}\bar{Y} \right] = 0 \quad (A-2)$$

where time varying excitations have been neglected. The static load has been ignored since motion about the equilibrium position is considered. Assume solutions of the form

$$\bar{X} = Ae^{i\Omega t}, \quad \bar{Y} = Be^{i\Omega t} \quad (A-3)$$

where the real part of the eigenvalues has been set equal to zero representing the threshold of stability. Substitution into equations (A-1) and (A-2) yields the following system of equations:

$$\begin{bmatrix} -(M'\Omega^2 - \bar{K}_{xx}) + i\Omega \bar{C}_{xx} & i\Omega \bar{C}_{xy} + \bar{K}_{xy} \\ i\Omega \bar{C}_{yx} + \bar{K}_{yx} & -(M'\Omega^2 - \bar{K}_{yy}) + i\Omega \bar{C}_{yy} \end{bmatrix} \begin{Bmatrix} \bar{X} \\ \bar{Y} \end{Bmatrix} = \{0\} \quad (A-4)$$

where $M' = \frac{mc\omega^2}{W}$.

Equating the real and imaginary parts of the coefficient matrix to zero gives

$$\Omega^2 = \left[\frac{(M'\Omega^2 - \bar{K}_{xx})(M'\Omega^2 - \bar{K}_{yy}) - \bar{K}_{xy}\bar{K}_{yx}}{\bar{C}_{xx}\bar{C}_{yy} - \bar{C}_{xy}\bar{C}_{yx}} \right] \quad (A-5)$$

$$\bar{D}^2 = M'\Omega^2 = \left[\frac{\bar{K}_{xx}\bar{C}_{yy} + \bar{K}_{yy}\bar{C}_{xx} - \bar{K}_{xy}\bar{C}_{yx} - \bar{K}_{yx}\bar{C}_{xy}}{\bar{C}_{xx} + \bar{C}_{yy}} \right] \quad (A-6)$$

Define the rigid rotor stability parameter, $\bar{\omega}_{tr}$, as

$$\bar{\omega}_{tr} = \bar{D}/\Omega = \sqrt{M'} = \omega \sqrt{\frac{m c}{W}} \quad (A-7)$$

Note that for the horizontal case where the rotor weight is the only external load on the bearing

$$W = m g$$

and equation (A-7) becomes

$$\bar{\omega}_{tr} = \omega \sqrt{\frac{c}{g}} \quad (A-8)$$

The linear bearing coefficients may be used to determine the stability threshold speed parameter, ω_{tr} , from equations (A-5), (A-6), and (A-7). Then, the speed, N_{tr} , at which the journal becomes unstable at the particular equilibrium eccentricity for which the bearing coefficients have been calculated may be determined from

$$N_{tr} = \bar{\omega}_{tr} \frac{30}{\pi} \sqrt{\frac{mc}{W}} \quad (\text{RPM}) \quad (A-9)$$

or

$$N_{tr} = \bar{\omega}_{tr} \frac{30}{\pi} \sqrt{c/g} \quad (\text{RPM}) \quad (A-10)$$

The above formulation assumes a rigid shaft. A flexible shaft threshold speed parameter, $\bar{\omega}_{tr}$, may also be calculated from [13].

$$\bar{\omega}_{tr} = \left[\bar{\omega}_{tr} \quad 1 + \bar{\omega}_{tr}^2 \Omega \left(\frac{g}{c\omega_{cr}^2} \right) \right]^{-1/2} \quad (A-11)$$

The disadvantage of this approximation is that the rigid bearing critical speed, ω_{cr} , must first be determined from a critical speed computer program. However, it is a relatively simple way to include the approximate effects of shaft flexibility in the bearing stability parameter.